

# Investigation of ultra-short-period W/C multilayers for soft X-ray optics

Fengli Wang (王凤丽), Zhanshan Wang (王占山), Shuji Qin (秦树基),  
Wenjuan Wu (吴文娟), Zhong Zhang (张众), Hongchang Wang (王洪昌), and Lingyan Chen (陈玲燕)

*Institute of Precision Optical Engineering, Tongji University, Shanghai 200092*

Received December 22, 2004

Ultra-short-period W/C multilayers having periodic thickness range of 1.15—3.01 nm have been fabricated for soft X-ray optics using the high vacuum direct current (DC) magnetron sputtering system. These multilayers were characterized by low-angle X-ray diffraction (LAXRD) and transmission electron microscope (TEM). The results show that the multilayer thin films with periodic thickness more than 1.5 nm have clear W-C interface and low roughness. But the structure of the periodic thickness below 1.5 nm is not clear. Finally, three ways to improve the performance of the multilayers are suggested.

OCIS codes: 220.0220, 230.0230, 310.0310, 340.0340.

The periodic multilayer has many interesting and useful mechanical, electrical, magnetic, and optical properties, which are related to either the coherent effect of modulation or the structure of thin films. The periodic multilayer mirrors are used for enhancing reflectivity in the wavelength range of 0.1—10 nm from grazing to normal incidence. Therefore, the multilayer reflectors have been used successfully in a range of applications, including extreme ultraviolet (EUV) lithography<sup>[1]</sup>, soft X-ray microscopy<sup>[2]</sup>, and soft X-ray astronomy<sup>[3]</sup>. The reflective efficiency of a multilayer mirror will be maximized when the individual layer is atomically flat, and the composition change at each interface atomically abrupt. However, the bonding nature between two materials may set limitations to such atomically distinct features. For example, there appears to have a tendency to form metallic carbide, which will lead to intrinsically rougher interface in W/C as opposed to W/B<sub>4</sub>C<sup>[4,5]</sup>. With the improvements of the fabrication and measurement technology, people<sup>[6,7]</sup> began to fabricate very thin films. After intensive research<sup>[8–14]</sup> into multilayer used in soft X-ray wavelength, W/C layer pair was chosen to fabricate the normal-incidence multilayers working in the wavelength range of 2.0—6.0 nm based on the practical experiment conditions. The purpose of this article is to investigate the fabrication technology of W/C multilayer using a direct current (DC) magnetron sputtering coater, especially in respect of the period thickness.

The samples used here were deposited on polished silicon(100) wafers (10 × 10 (mm)) using a high vacuum DC magnetron sputtering coater JGP560CIV. Figure 1 is the inner structure schematic diagram of vacuum chamber. There are four magnetrons which are uniformly arranged along the circularity, and the targets with 100-nm diameter face upward. The substrate facing downward is mounted on a spin platen driven by a step motor, which is mounted on a rotor plate driven by another step motor, the vertical distance from target to substrate can be adjusted from 50 to 150 mm, here it is set to 80 mm for both targets. The substrate can move to any position controlled by computer or by manually operation, it can spin while rotating with the

rotor plate. The spin rate was held at approximately 5 rpm to make the coating more uniform, and the rotation rate was set to 2 rpm. When a substrate in spin motion stays over a magnetron target, one layer is deposited, then it moves to another target to fabricate next layer. Each layer thickness can be accurately controlled by the stay time over each target if all operation parameters are kept constant during deposition. In these experiments, a planar W target with 99.99% purity and a C target with the same purity were used and mounted on the magnetrons A and C respectively. The background pressure in the vacuum chamber before deposition was lower than  $5.0 \times 10^{-5}$  Pa in all cases, and

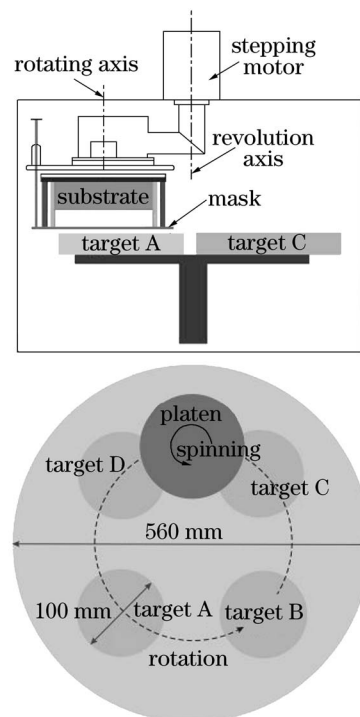


Fig. 1. Inner structure schematic diagram of vacuum chamber for the magnetron sputtering system.

**Table 1. Parameters of the W/C Samples**

Sample	1	2	3
Periodic Number (N)	40	100	300
Nominal Period (nm)	3.00	1.80	1.20
Measured Period (XRD) (nm)	3.01	1.70	1.15

the pressure of argon gas with 99.99% purity was maintained at  $0.81 \pm 0.01$  Pa during deposition. The targets of W and C operated at constant powers mode, and the powers are 25 and 130 W respectively. At the same time, a negative substrate bias, 200 V, was used during deposition. The sputtered rates of W and C, calculated based on the time of the substrate over each target and the periodic thickness determined by X-ray diffraction (XRD) measurements, were 0.1202 nm/s for W and 0.0428 nm/s for C respectively. The parameters of the samples described here are summarized in Table 1.

As a complementary technique, the  $\theta$ - $2\theta$  scan of XRD for three multilayer samples was used before the samples were cut to cross-section for transmission electron microscope (TEM) observation. The structural information obtained by XRD is an average over a wide region of the specimen, while it is obtained from a more local area of the specimen by electron diffraction (ED). In this article, these two methods were used to characterize the deposited W/C multilayers.

The periods of W/C multilayers were determined by low angle X-ray diffraction (LAXRD,  $2\theta \leq 15^\circ$ ) at Cu  $K_\alpha$  line ( $\lambda = 0.154$  nm). The period is given by<sup>[15]</sup> the corrected Bragg equation

$$\sin^2 \theta = \left( \frac{n\lambda}{2d} \right)^2 + 2\delta, \quad (1)$$

where  $\theta$  is the angle of peak position,  $n$  is the order of reflection,  $\lambda$  is the X-ray wavelength, and  $1 - \delta$  is the real part of average index of refraction for a multilayer. The value of  $\delta$  is  $\sim 3 \times 10^{-5}$  typically, which only leads to significant deviations from Bragg's law when  $2\theta$  values are less than  $3^\circ$  for Cu  $K_\alpha$  line. The XRD spectrometer used here is made in Japan. Figure 2 shows the measured results, the curves are directed by the arrows labelled 1 and 2 which are the first section and second section of the whole curve sublevel measured by XRD because the diffraction intensity of the XRD is not enough at high incident angle, through changing the tilt to enhance the intensity. Each angle ( $2\theta$ ) of the Bragg peaks was shown in the figure. The relatively sharp Bragg peaks of three samples show that the layer structure is good and the deposition process is stability. Table 1 shows the calculated period using Eq. (1) for each multilayer.

TEM and ED were used to obtain the micro-structural information on the composition profile perpendicular to the layers. TEM experiments were performed on a Philips CM 200 operating at 160 kV. The cross-sectional specimens for TEM observation and ED were prepared by ion-beam thinning and observed with the electron beam incident parallel to the interfaces.

From the TEM measurement, the direct image of the layer structure could be obtained. The typical bright-field images of three specimens are shown in Figs. 3(a), (b), and (c) respectively. The bottom of the figures is

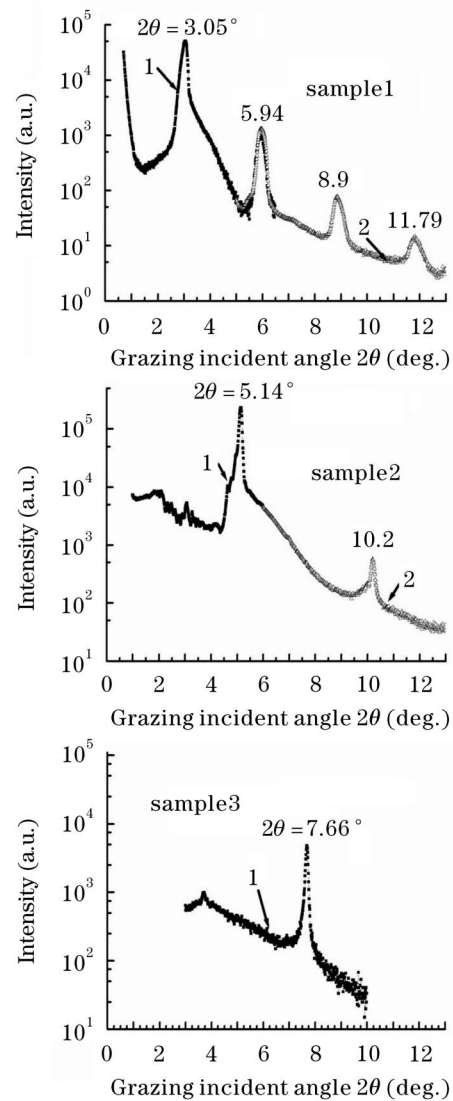


Fig. 2. XRD measurements of periodic W/C multilayers, respectively for period of  $d = 3.01$  nm (sample1), 1.70 nm (sample2) and 1.15 nm (sample3).

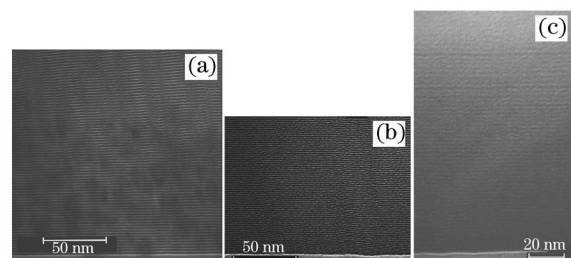


Fig. 3. TEM bright-field images from cross-sectional specimens of high-Z/low-Z multilayer films: (a) sample1, (b) sample2, (c) sample3.

substrate Si(100), the dark lines are corresponding to the W layers, while the bright ones the C layers. Figure 3(a) and (b) show well-formed layer structures for two samples. It is evident that both W and C layers are in amorphous phases. In addition, the W-C interfaces for W/C multilayers appear to be sharp. Figure 3(c) also shows a layer structure for sample3, but the interfaces is not sharp. From the selected electron diffraction,

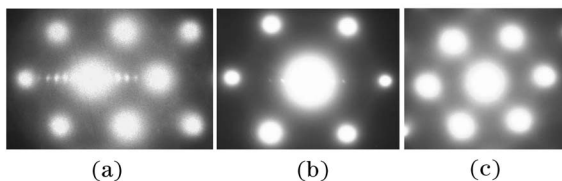


Fig. 4. Electron diffraction patterns of cross-sectional multilayer near the transmitted beam: (a) sample1, (b) sample2, (c) sample3.

there are several orders of visible satellite spots at least for sample1 and sample2, as illustrated in Figs. 4(a) and (b). The image near the zero beam in their electron diffraction patterns shown is taken from the same areas as Figs. 3(a) and (b). This means that both sample1 and sample2 have good periodicity in real space. However, there is not clear layer structure for sample3 from Fig. 4(c).

There is also some information about deposition process obtained from Fig. 2. When the substrate has a rough surface, the multilayer near substrate side does not have a sharp W-C interface. However, the coatings become more and more flat with the increment of layer number. This phenomenon indicates that the more of the layer number, the better of the multilayer feature, as reported in Ref. [8]. Furthermore, the ratio  $\Gamma$  of metal layer thickness to period for sample1 is found to be about 0.6, which is significantly larger than the value of  $\Gamma = 0.4$  predicted from the deposition rates. This indicates that carbide has been formed in the multilayer structure, as observed previously in W/C system<sup>[5,11]</sup>.

The results indicate that the ultra-short-period multilayer can be realized. The period structure with a smaller period thickness ( $< 1.5$  nm) is not better than the one with a bigger period thickness in performance, but further improvements of various ultra-short-period multilayer would result in the development of more practical implementations. There may be three ways to further improve the quality of multilayers. Firstly, increasing the number of periods will almost result in increased reflectivity (the maximum useful number of period in these films is essentially  $N = 600$ ). Secondly, the assumption of pure W and C layers having a bulk density is incorrect at some level of detail. More accurate modelling of the microstructure, particularly the composition

and density of the extended W-rich layers, may further make the value of  $\Gamma$  optimal because  $\Gamma$  may depend on the period. Finally, it will be helpful to use the materials with a greater optical contrast, lower absorption, and (or) smaller interface widths, such as  $W/B_4C$ .

This work was supported by the National Natural Science Foundation of China (No. 10435050, 60378021), and by the Nanometer Technology Special Foundation of Shanghai Science and Technology Committee (No. 0352nm090). F. Wang's e-mail address is wfl95711@sohu.com.

## References

1. A. M. Haeryluk and L. G. Seppala, *J. Vac. Sci. Technol. B* **6**, 2162 (1988).
2. D. L. Shealy, R. B. Hoover, T. R. Barbee, and A. B. C. Walker, *Opt. Eng.* **29**, 721 (1990).
3. L. Golub, M. Herant, K. Kalata, I. Lovas, G. Nystrom, F. Pardo, E. Spiller, and J. Wilczynski, *Nature* **344**, 842 (1990).
4. A. F. Jankowski and D. M. Makowiecki, *Proc. SPIE* **984**, 64 (1988).
5. A. F. Jankowski, L. R. Schrawyer, M. A. Wall, W. W. Craig, R. I. Morales, and D. M. Makowiecki, *J. Vac. Sci. Technol. A* **7**, 2914 (1989).
6. D. L. Windt, E. M. Gullikson, and C. C. Walton, *Opt. Lett.* **27**, 2212 (2002).
7. J. F. Seely, G. Gutman, J. Wood, G. S. Herman, M. P. Kowalski, J. C. Rife, and W. R. Hunter, *Appl. Opt.* **32**, 3541 (1993).
8. A. F. Jankowski, *Opt. Eng.* **29**, 968 (1990).
9. E. Spiller and L. Golub, *Appl. Opt.* **28**, 2969 (1989).
10. M. Arbaoui, R. Barchewitz, C. Sella, and K. B. Youn, *Appl. Opt.* **29**, 477 (1990).
11. Z. Jiang, V. Dupuis, B. Vidal, M. F. Ravet, and M. Piecuch, *J. Appl. Phys.* **72**, 931 (1992).
12. D. G. Stearns, R. S. Rosen, and S. P. Vernon, *Opt. Lett.* **16**, 1283 (1991).
13. D. G. Stearns, R. S. Rosen, and S. P. Vernon, *J. Vac. Sci. Technol. A* **9**, 2662 (1991).
14. A. E. Yakshin, I. I. Khodos, I. M. Zhelezniak, and A. I. Erko, *Opt. Commun.* **118**, 133 (1995).
15. P. F. Miceli, D. A. Neumann, and H. Zabel, *Appl. Phys. Lett.* **48**, 24 (1986).